1997

A study of wind stress determination methods from a ship and an offshore tower

Frederickson, Paul A.; Davidson, Kenneth L.; Edson, James B.

Journal of Atmospheric and Oceanic Technology, Volume 14, pp. 822-834.
http://hdl.handle.net/10945/41315

A Study of Wind Stress Determination Methods from a Ship and an Offshore Tower*

PAUL A. FREDERICKSON AND KENNETH L. DAVIDSON
Department of Meteorology, Naval Postgraduate School, Monterey, California

JAMES B. EDSON
Applied Ocean Physics and Engineering Department, Woods Hole Oceanographic Institution, Woods Hole, Massachusetts

(Manuscript received 25 May 1996, in final form 29 January 1997)

ABSTRACT

Comparisons are made between surface wind stress measurements obtained by the inertial-dissipation and direct covariance methods on a stable offshore tower and by the inertial-dissipation and bulk methods on a ship. The shipboard inertial-dissipation friction velocity measurements agreed very well with both the tower inertial-dissipation and direct covariance values, to within ±2% in the mean and with a 10% or lower rms scatter. The inertial-dissipation determinations also exhibited less scatter than the tower direct covariance measurements. A detailed error analysis indicates that shipboard inertial-dissipation wind stress values can have an accuracy of better than 15% in near-neutral conditions, as compared to an accuracy of roughly 30% for the bulk method. The accuracy of shipboard inertial-dissipation values was shown to be equal to that of direct covariance measurements from a tower. Errors in inertial-dissipation wind stress values are most likely due primarily to deviations from the assumed balance between turbulent kinetic energy production and dissipation and to errors in determining the wind speed variance spectra. Errors in direct covariance measurements are most likely due primarily to finite time averaging and to flow distortion effects, unless great care is taken to minimize or correct for flow distortion. The high accuracy of inertial-dissipation wind stress values found in this study, combined with the well-known difficulties in shipboard direct covariance measurements due to platform motion and flow distortion, demonstrate that the inertial-dissipation method is the best option at present for determining the wind stress from a ship.

1. Introduction

An understanding of the complex interactions between the ocean and atmosphere is critical in many areas of geophysical study. For instance, the momentum flux across the atmosphere–ocean interface, often referred to as the surface wind stress, is the primary forcing mechanism for ocean waves, currents, and near-surface turbulence. In the past, measurements of the wind stress have been made on ships, fixed platforms, buoys, and aircraft. The value of obtaining measurements from a ship is that it can move to study different areas encompassing varied oceanic, hydrographic, and atmospheric conditions, including open-ocean areas where platforms and buoys are generally not available. The method most often used to measure the wind stress from a ship is the inertial-dissipation method (see, e.g., Pond et al. 1971; Khalsa and Businger 1977; Large and Pond 1981; Anderson 1993; Yelland and Taylor 1996). This method has an important advantage over the direct covariance method, in that it is based on high-frequency wind measurements that are unaffected by platform motion. In addition, the inertial-dissipation method is more direct than bulk methods, which depend only upon mean measurements, since it is based on an actual wind turbulence statistic.

In order to examine the validity of the inertial-dissipation method, comparisons have been made between wind stress measurements on ocean platforms by the inertial-dissipation method and the more widely accepted direct covariance method. Large and Pond (1981) compared 192 inertial-dissipation and covariance friction velocity measurements from a tower in deep water and found a difference between the two methods of only 4% in the mean and less than a 20% difference in nearly all cases. Geernaert et al. (1988) observed close agreement between inertial-dissipation and covariance wind stress values under near-neutral conditions and poorer agreement in stable conditions. Edson et al. (1991) found significantly better agreement between inertial-dissipation and covariance wind stress measurements from a well-exposed sensor than from a poorly exposed sensor on a tower and concluded

*HEXOS Contribution Number 51.

Corresponding author address: Paul A. Frederickson, Department of Meteorology, Naval Postgraduate School, 589 Dyer Road, Room 254, Monterey, CA 93943-5114.
E-mail: 5196p@vml.cc.nps.navy.mil

that the inertial-dissipation method was much less affected by flow distortion than the covariance method.

Comparisons between simultaneous shipboard inertial-dissipation wind stress determinations and direct covariance measurements from a nearby tower have been rare or nonexistent in the past. However, several studies, including those by Smith et al. (1992), Anderson (1993), and Yelland and Taylor (1996), have found that drag coefficient formulations determined from shipboard inertial-dissipation measurements generally agree well with previously determined direct covariance formulations from towers. These results indicate that shipboard inertial-dissipation wind stress measurements agree well in the mean with direct covariance measurements from fixed ocean towers.

In October and November of 1986 the Humidity Exchange over the Sea (HEXOS) Main Experiment (HEXMAX) was conducted in the North Sea off the coast of the Netherlands. During HEXMAX, measurements of the surface wind stress were made from both a research vessel, the RRS *Frederick Russell,* and a research platform, Meetpost Noordwijk (MPN). Wind stress values were obtained using the inertial-dissipation and bulk methods on the *Frederick Russell,* and the inertial-dissipation and direct covariance methods on MPN. During almost half of the HEXMAX experiment the *Frederick Russell* operated nearby the MPN tower. This dataset is believed to be the only one available with extensive simultaneous wind stress measurements from a ship and a fixed tower in close proximity to each other. The objective of this study is to determine the accuracy of shipboard inertial-dissipation wind stress measurements relative to other methods and platforms by comparing the ship and tower measurements and estimating the errors associated with the different wind stress determinations.

2. Theoretical background

a. Direct covariance method

The wind stress caused by turbulent eddies τ is defined as

$$\tau = -\rho\langle u'w'\rangle, \tag{1}$$

where ρ is the air density, u' and w' are the turbulent components of streamwise and vertical wind velocity, respectively, and the brackets denote an average over an infinite ensemble. In practice, when using the direct covariance method to estimate the wind stress, the ensemble average is approximated by averaging simultaneous measurements of u' and w' cross correlated over a finite time interval. The accuracy of this approximation generally increases with the length of the averaging interval, as long as conditions remain near stationary. Other factors that can cause errors in direct covariance wind stress measurements include flow distortion effects, sensor accuracy, imperfect vertical alignment of the sensor, and platform motion contamination of the wind measurements.

b. Inertial-dissipation method

In the atmospheric surface layer, the wind stress can be expressed according to the Monin–Obukhov (MO) wind speed scaling parameter, known as the friction velocity u_*, by the expression

$$\tau = \rho u_*^2. \tag{2}$$

When using the inertial-dissipation (ID) method, it is usually assumed that a balance exists between the viscous dissipation of turbulent kinetic energy (TKE) ε and the buoyant and shear production of TKE. By also assuming that conditions are steady state and horizontally homogeneous, the dimensionless TKE equation for the atmospheric surface layer can be solved for u_*, resulting in

$$u_* = \left[\frac{\varepsilon kz}{\Phi_M(z/L) - z/L}\right]^{1/3}, \tag{3}$$

where k is von Kármán's constant [taken to be 0.4, after the review by Frenzen and Vogel (1995)], z is the height above the surface, and Φ_M is the dimensionless wind profile function. In this study we have used the wind profile function determined by Edson et al. (1991) to provide the best fit between HEXMAX MPN inertial-dissipation and covariance wind stress values. Here L is the MO length scale, defined as

$$L = \frac{T_v u_*^2}{kg(T_* + 0.61Tq_*)}, \tag{4}$$

where T_v is the virtual temperature, g is the acceleration of gravity, and T_* and q_* are the MO surface-layer scaling parameters for temperature and humidity, respectively.

By assuming the existence of locally isotropic turbulence within the inertial subrange and by invoking Taylor's "frozen" turbulence hypotheses, the rate of dissipation of TKE can be related to the wind speed variance spectrum $S_u(f)$, according to

$$\varepsilon = 2\pi\alpha^{-3/2}S_u(f)^{3/2}f^{5/2}U_{\rm rel}^{-1}, \tag{5}$$

where α is the Kolmogorov constant (taken to be 0.55 in this study), f is the frequency, and $U_{\rm rel}$ is the wind speed relative to the sensor. With measurements of the wind speed at frequencies within the inertial subrange, ε can be obtained via Eq. (5), enabling u_* to be determined by an iterative process from Eqs. (3) and (4).

A potential source of error in employing the ID method arises from the assumption of a balance existing between TKE production and dissipation. Several studies have shown this assumption to be approximately true for weakly unstable surface layers (Garratt 1972; McBean and Elliott 1975; Bradley et al. 1981; Oncley et al. 1995). However, other experiments have found that the rates of dissipation of TKE were too large to balance production (Pond et al. 1971; Wyngaard and Cote 1971; McBean et al. 1971; Champagne et al. 1977; Hogstrom 1990; Edson et al. 1991), while several recent studies have observed dissipation rates that are too small to balance production (Frenzen and Vogel 1992; Vogel and Frenzen 1992; Fairall and Edson 1994; Oncley et al. 1996). This summary is presented to illustrate the point that current knowledge of the terms in the TKE budget is still very incomplete.

An ''effective'' Kolmogorov constant α_e can be used when employing the ID method to account for any imbalance between TKE production and dissipation. The constant α_e is defined by explicitly assuming a TKE balance and is determined by finding the value of α that provides the best fit between concurrent ID and direct covariance u_* values. The effective constant will be equal to the true Kolmogorov constant only if a balance exists between TKE production and dissipation. Deacon (1988) summarized the results of 10 studies and found an average value for α_e (after conversion to $k = 0.4$, as used in this study) of 0.58 ± 0.025. Recently, Hogstrom (1990) obtained a value of 0.6 for α_e, while Edson et al. (1991) found a value of 0.55 from the HEXMAX MPN data. Hogstrom (1996) concluded from a summary of 32 previous studies that the best estimate for the true value of α was 0.52 ± 0.02. Therefore, effective Kolmogorov values have generally been found to be slightly higher than the true values, indicating that TKE dissipation usually exceeds production in the atmospheric surface layer (Hogstrom 1996).

The use of an effective Kolmogorov constant to improve the accuracy of the ID method is problematic, however, since concurrent covariance measurements are generally not available, and, in any case, the goal is to have confidence in independent ID wind stress determinations. The large variation in published α_e values makes it impossible to assume a specific value for α_e under given conditions to improve the accuracy of individual ID wind stress determinations. Perhaps the best that can be expected at present is to use a value for α_e falling in the middle of the range of published effective and true values, such as 0.55, as used in this study and by Large and Pond (1981), Edson et al. (1991), Anderson (1993), and Yelland et al. (1994). Assuming that the value of α_e that should be used under any given conditions lies in the range between 0.5 and 0.6, the maximum resulting error in u_* due to using a value of 0.55 is about 5% in near-neutral conditions. This approximates the largest error likely to result in ID u_* values due to deviations from a TKE balance under near-neutral stability. With improved knowledge of α_e and of the terms in the TKE budget, however, future ID wind stress determinations should have improved accuracy.

c. The bulk aerodynamic method

When employing the bulk method, the wind stress is parameterized in terms of the mean wind speed by using a bulk drag coefficient C_D, according to the formula

$$\tau = \rho C_D(z)[U(z) - U_o]^2, \qquad (6)$$

where $U(z)$ is the mean wind speed at the measurement height z above the surface and U_o is the mean speed of the ocean surface. The drag coefficient over the ocean surface has been found by many studies to increase with wind speed, and a common first-order parameterization is to linearly relate the 10-m neutral drag coefficient (C_{DN10}) to the 10-m neutral wind speed (U_{N10}) (e.g., Large and Pond 1981; Smith et al. 1992; Anderson 1993). In this study we used the following HEXMAX relationship presented by Smith et al. (1992):

$$10^3 C_{DN10} = 0.27 + 0.116 U_{N10}, \qquad (7)$$

which is valid for neutral wind speeds from 5 to 25 m s^{-1}. This formulation was determined by averaging the neutral linear regressions between direct covariance C_{DN10} and U_{N10} measurements from three different sensors (sonic, K-Gill, and pressure anemometers) on the MPN tower during HEXMAX. Note that these measurements were corrected for the surface current and that Eq. (7) was determined independent of the MPN covariance measurements used in this study. The neutral drag coefficient given in Eq. (7) was adjusted for stability effects and height differences in order to determine u_* values by equating Eqs. (2) and (6). Bulk estimates of L, necessary to perform this adjustment, were obtained using a wind speed-independent value of 1.1×10^{-3} for the near-neutral transfer coefficients for sensible heat (C_{TN10}) and moisture (C_{QN10}) (e.g., Garratt 1992; Kraus and Businger 1994).

Bulk drag coefficients are generally determined by averaging covariance or inertial-dissipation measurements from towers or ships in a particular location and over a specific time period. The drag coefficient therefore describes the average sea surface roughness conditions for that specific site and time period. Errors in bulk wind stress determinations can be caused by errors in the original measurements used to derive the drag coefficients. Errors can also be due to differences between the average air–sea conditions that occurred at the original measurement site during the time period the bulk formulation was determined, and the conditions occurring at the particular location and time the bulk formulation is being applied. These errors can be due to such factors as frontal passages, wind shifts, surface slicks, and differences in water depth, fetch, and wave field, for example.

3. Measurements and data analysis

a. Meetpost Nordwijk platform

The Meetpost Nordwijk (MPN) platform is located in the North Sea, approximately 9 km off the Dutch coast in a mean water depth of approximately 18 m. Wind stress values were determined by the covariance and inertial-dissipation methods on MPN using wind measurements from a Kaijo Denki sonic anemometer. Inertial-dissipation estimates of the wind stress were computed iteratively using inertial-dissipation values of T_* (from the sonic anemometer/thermometer) and q_* (from a Lyman-alpha hygrometer) to determine L. All sensors were located at the tip of a boom extending 16 m outward on the west side of the platform, at a height of 5–8 m above the sea surface. The length of the boom was chosen as the minimum necessary to reduce the effects of flow distortion caused by the tower, as determined from wind tunnel tests. The averaging interval of the measurements varied between 19.4 and 36.6 min, and the mean interval was 29.4 min. Bulk u_* values were not computed for the tower because surface current speed data were not available for this analysis, and the large currents observed at the MPN site (up to 1 m s^{-1}) could not be neglected without the possibility of large errors. The instruments and procedures employed in obtaining wind stress measurements at MPN are discussed in detail by Fairall et al. (1990).

The MPN direct covariance measurements were carefully corrected for flow distortion effects. First, the well-known tilt correction was performed, then a potential-flow model for wind covariance distortions around simplified geometric objects was used to apply corrections to the covariance measurements. These flow distortion corrections are described by Oost et al. (1994). The application of these corrections brought the covariance measurements into much better agreement with the inertial-dissipation u_* measurements, which were not corrected for flow distortion.

b. RRS Frederick Russell

Measurements on the *Frederick Russell* (FR) were obtained by personnel from the Naval Postgraduate School (NPS), Monterey, California, and the Institute of Oceanographic Sciences (IOS), Wormley, United Kingdom. The NPS group used hot-films to measure wind turbulence, and the IOS group measured the mean vector wind using a propeller-vane anemometer, and the air temperature and humidity using an aspirated psychrometer. In order to minimize the ship's influence on the measurements, the sensors were mounted on a well-exposed 10-m mast located 2 m aft of the bow (Fig. 1). The propeller-vane anemometer and psychrometer were located atop the mast, 14.5 m above the sea surface, and the hot-film was mounted on the lower arm of the mast, 13 m above the sea surface. The sea surface temperature was measured with a towed skimming thermister. The ship's speed through the water, necessary to determine the true wind speed, was measured by the FR's electromagnetic speed log.

Wind speed variance spectra were obtained from the hot-film anemometer measurements, which were sampled at a 50-Hz rate. The hot-film voltage-to-wind speed calibrations were computed and applied during post-processing because the calibrations change as the hot-film ages. The wind speed variance spectra were averaged over 10-min intervals and the slope of each averaged spectra with respect to frequency was checked in logarithmic space to ensure it was close to $-5/3$, as predicted for isotropic turbulence in the inertial subrange [Eq. (5)]. Those spectra that did not exhibit a $-5/3$ slope were excluded from the data analysis. The frequency-normalized spectra were then averaged over an appropriate frequency band within the inertial subrange (approximately 2–10 Hz, depending upon wind speed). Inertial-dissipation friction velocity values were computed by an iterative process using averaged wind variance spectra and bulk estimates of T_* and q_*, which were computed from the mean air–sea temperature and humidity data in order to determine L. Bulk u_* values were determined by an iterative process from the mean wind speed and air–sea temperature and humidity measurements. Since the ship's true wind speed was determined relative to the ocean surface, the surface speed U_o could be neglected in Eq. (6) when determining bulk u_* values.

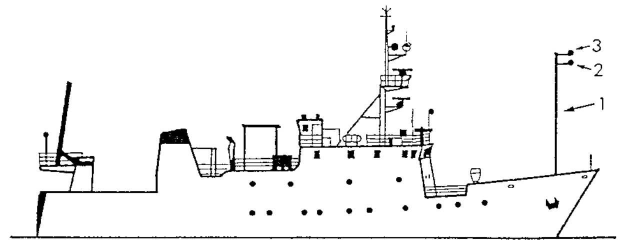

FIG. 1. The RRS *Frederick Russell,* showing location of 1) 10-m meteorology mast; 2) lower arm, holding NPS hot-film anemometers; 3) upper arm, holding IOS mean wind, temperature, and humidity sensors.

To examine the effects of flow distortion on the wind turbulence measurements, the ratio of the ID u_* values over the bulk values was plotted versus the wind direction relative to the FR's bow (Fig. 2). If we assume that during the entire experiment the average sea surface roughness and atmospheric stability conditions encountered were similar when the wind was from different relative directions, then this ratio should be nearly constant with relative wind direction if there were no effects from flow distortion on the turbulence measurements. From Fig. 2 it can be seen that for relative wind directions within $-20°$ to $+30°$ clockwise from the ship's bow, the average ratio is nearly constant, only varying by less than 2%. This indicates that within this relative wind direction range, the effects of flow distortion are minimal, and consequently only the data within this range were used in our analysis. Since the FR was steaming with its bow into the wind during most of the experiment, only a small percentage of ship data were excluded due to unfavorable wind directions.

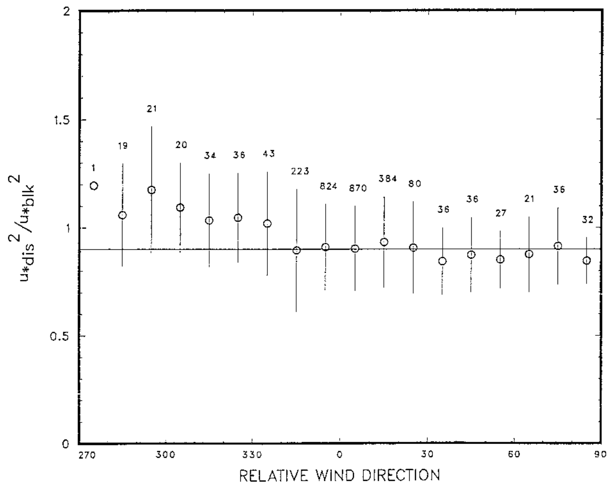

FIG. 2. Ratio of inertial-dissipation over bulk u_*^2, estimates from the *Frederick Russell* versus relative wind direction, in degrees clockwise from the bow. Error bars show the standard deviation and the number of data points in each bin is labeled.

c. Combined ship and tower data

During postprocessing, the FR 10-min data were block averaged into 30-min values, which were then paired with the closest simultaneously measured MPN data. Since the starting times of the ship and tower measurements were different and the lengths of the averaging intervals varied on the tower, the amount of time overlap between data pairs varied. Each pair of ship and tower values used for comparison had at least a 50% overlap in time, and the average overlap was 74%. The winds were from an unfavorable direction to obtain turbulence measurements on the MPN boom during most of the time the FR was in the vicinity of the tower, with the result that only 69 pairs of ship and tower measurements were available for comparison.

A summary of the measurements from the two platforms during the comparison periods is presented in Table 1. The wind speeds were generally moderate, ranging from roughly 5 to 15 m s^{-1}, and the air–sea temperature differences varied from about $-3°$ to 2°C. Weakly unstable stratification was observed during most comparison periods: 70% of the MPN ID z/L values were in the range between -0.116 and -0.005, and 70% of the FR ID z/L values were in the range between -0.125 and -0.005.

4. Friction velocity comparisons

a. Comparison methods

In this section the performance of different wind stress measurement methods and platforms is compared by assuming that there should exist an exact linear relationship between two u_* populations but that systematic and random errors introduce scatter into both measurements being compared. Therefore, the comparisons conducted in this section include both linear regression analyses and an examination of the scatter between the two populations.

TABLE 1. Summary of the ship (FR) and tower (MPN) measurements during the comparison periods, obtained by the inertial-dissipation (ID), bulk, and direct covariance (DC) methods.

Measured parameter	Platform and method	Mean value	Min value	Max value
U_{10} (m s^{-1})	FR	9.4	4.8	14.3
	MPN	9.2	4.6	15.2
$T_{10} - T_{sea}$ (°C)	FR	-0.7	-2.3	1.8
	MPN	-0.6	-2.8	2.1
z/L (z = 10 m)	FR ID	-0.068	-0.392	0.035
	FR bulk	-0.059	-0.463	0.028
	MPN ID	-0.060	-0.345	0.044
	MPN DC	-0.055	-0.370	0.244
u_* (m s^{-1})	FR ID	0.345	0.159	0.591
	FR bulk	0.358	0.150	0.627
	MPN ID	0.345	0.161	0.610
	MPN DC	0.340	0.144	0.638

It was considered undesirable to use a standard linear regression when comparing two independent u_* populations, since it must be assumed that one population is the dependent variable. Therefore, when comparing two u_* populations obtained by different methods or on different platforms, "neutral" linear regressions were computed. This was done by computing two regressions, with both u_* populations in turn being used as the dependent variable, and then averaging the two resulting regression lines together. The slope and y intercept of the neutral regression line and the linear correlation coefficient between the two u_* populations were computed.

The percentage difference between two u_* populations, D, was computed by determining the mean of the ratio of the difference between two u_* values over their average value, and expressing as a percentage

$$D = 100 \times \frac{1}{N}\sum_{i=1}^{N}\frac{(X_i - Y_i)}{(X_i + Y_i)/2}, \qquad (8)$$

where X is the u_* population listed at the top of the columns in Table 2, Y is the u_* population listed to the left of the rows, and N is the number of data pairs in the comparison. This statistic is useful for determining how well two u_* populations agree in the mean.

The "observed" scatter O was computed by expressing the root-mean-square difference between two u_* populations as a percentage of the mean of the two populations

$$O = 100 \times \frac{\left[\frac{1}{N}\sum_{i=1}^{N}(X_i - Y_i)^2\right]^{1/2}}{(\overline{X} + \overline{Y})/2}, \qquad (9)$$

where X, Y, and N are as defined above. This statistic

TABLE 2. Summary of the friction velocity comparisons for the ship (FR) and tower (MPN) platforms and the inertial-dissipation (ID), bulk, and direct covariance (DC) methods. All statistics are defined in section 4a, except for P and X%, Y% of P, which are defined in section 5.

	Parameter X		
Parameter Y	MPN ID	FR ID	FR bulk
MPN DC			
Regression slope	1.014	0.968	0.923
Reg. y intercept (m s^{-1})	−0.010	0.006	0.010
Correlation coefficient	0.975	0.961	0.965
$X - Y$ percentage diff. D	1.8	1.3	4.9
Observed scatter O (%)	7.6	9.6	10.7
Predicted scatter P (%)	7.7	9.5	10.9
X%, Y% of P	17, 83	36, 64	52, 48
MPN ID			
Regression slope		0.955	0.911
Reg. y intercept (m s^{-1})		0.016	0.019
Correlation coefficient		0.981	0.977
$X - Y$ percentage diff. D		−0.6	3.0
Observed scatter O (%)		6.7	8.6
Predicted scatter P (%)		6.8	8.9
X%, Y% of P		60, 40	76, 24
FR ID			
Regression slope			0.954
Reg. y intercept (m s^{-1})			0.004
Correlation coefficient			0.984
$X - Y$ percentage diff. D			3.6
Observed scatter O (%)			7.3
Predicted scatter P (%)			7.6
X%, Y% of P			63, 37

is useful as a measure of the scatter between two u_* populations and provides insight into the magnitude of the combined errors in the u_* values being compared.

b. Comparison results

Scatterplots of the friction velocity comparisons are presented in Fig. 3–8, and the comparison statistics are summarized in Table 2. The comparison of inertial-dissipation and covariance u_* values measured on the MPN tower is presented in Fig. 3. This comparison is essentially a test of the ID method, since the same sonic anemometer measuring over the same time periods was used for both methods. The one-to-one linear relationship between the two populations is very strong and the percent difference of 1.6% and observed scatter of 7.6% are very small. The good mean agreement is expected, since the effective Kolmogorov constant and dimensionless wind profile function used in computing the ID values were determined explicitly by finding the best agreement between the two methods during HEXMAX. The small scatter indicates that the effects of flow distortion have been properly corrected for in the covariance measurements. The excellent agreement between the MPN ID and covariance u_* values demonstrates that both methods are useful for measuring the wind stress at sea when the effects of flow distortion can be taken into account and platform motion is not a factor.

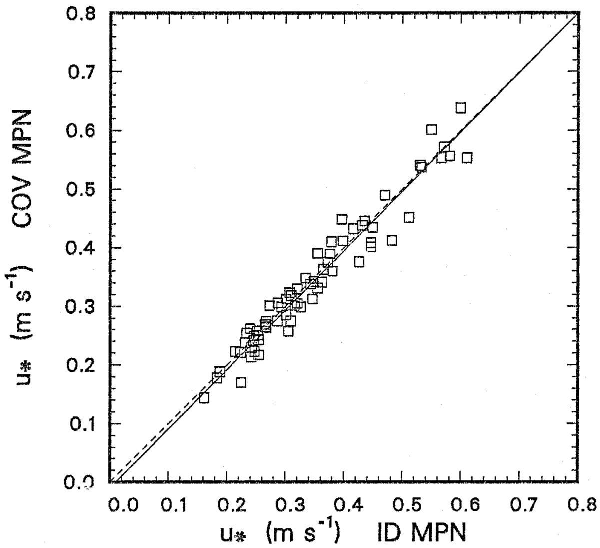

FIG. 3. Scatterplot of MPN direct covariance versus MPN inertial-dissipation u_* values. Solid line is the neutral regression line between the two populations; dashed line is one-to-one correspondence line.

Figures 4 and 5 show the comparisons between the FR ID friction velocity values and the MPN covariance and ID values, respectively. The FR ID u_* measurements agree extremely well with the MPN covariance and ID values, having a mean agreement of better than ±2% and an observed scatter of less than 10% in both cases. Although the linear relationships in these two comparisons are similar, the observed scatter between the FR and MPN ID u_* values (6.7%) is much smaller than the FR ID and MPN covariance comparison (9.6%). The observed scatter between the FR and MPN ID u_* values (6.7%) is even less than for the intercomparison

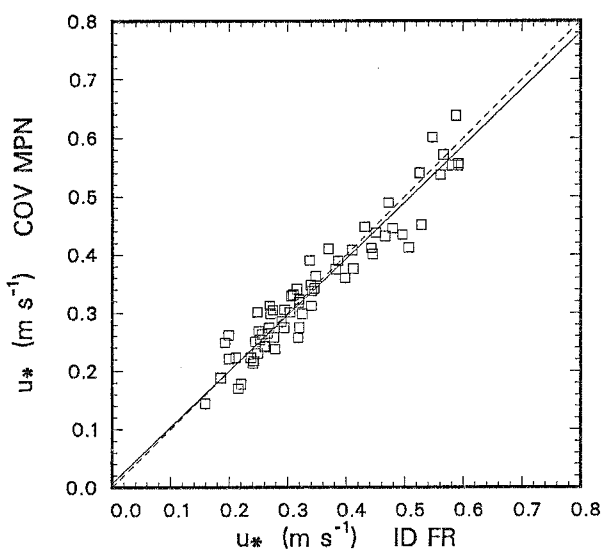

FIG. 4. As in Fig. 3 except for MPN direct covariance versus FR inertial-dissipation u_* values.

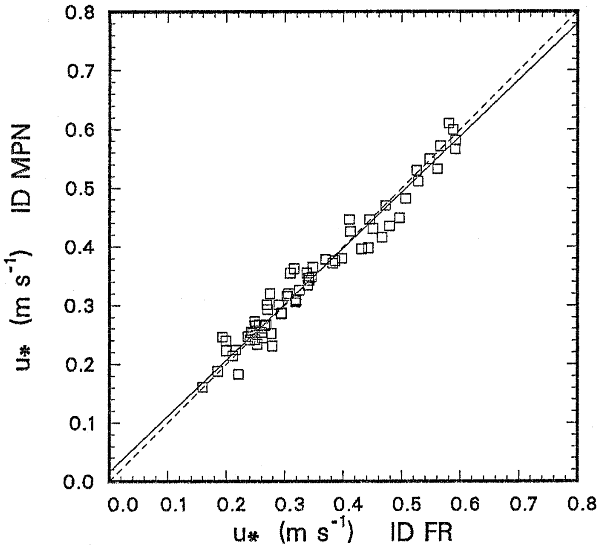

FIG. 5. As in Fig. 3 except for MPN inertial-dissipation versus FR inertial-dissipation u_* values.

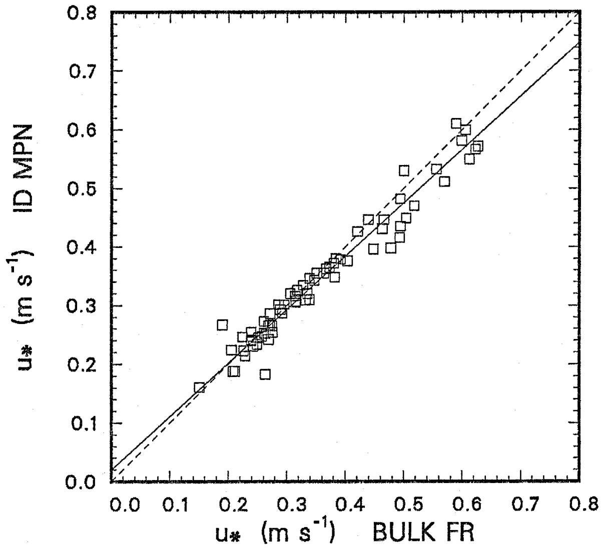

FIG. 7. As in Fig. 3 except for MPN inertial-dissipation versus FR bulk u_* values.

of MPN ID and covariance values (7.6%). This result is somewhat surprising, considering that 1) different sensors mounted on very different platforms were used for the two measurements, 2) the ship was operating several kilometers away from the tower, and 3) the starting and ending times of the measurements were different for the ship and tower values. The FR versus MPN ID comparison most likely has less scatter than the MPN intercomparison because the same method of determining u_* was used on both platforms. The close agreement between the ship ID and the tower covariance and ID u_* values demonstrates that the wind stress can be measured by the inertial-dissipation method on a ship with a high degree of accuracy.

Comparisons between the FR bulk u_* values and the MPN ID and covariance values are presented in Figs. 6 and 7, respectively. In both cases the FR bulk u_* values exhibit a poorer one-to-one agreement and greater scatter than the corresponding FR ID comparisons with the MPN values. This occurred despite the fact that the neutral drag coefficient used to compute the FR bulk u_* values was determined from covariance measurements made on MPN during HEXMAX. The comparison between the FR bulk and ID u_* values is presented in Fig. 8. The linear agreement is better and the scatter

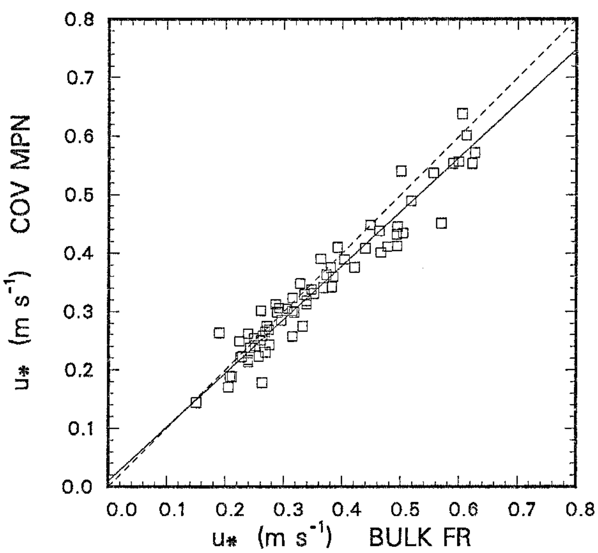

FIG. 6. As in Fig. 3 except for MPN direct covariance versus FR bulk u_* values.

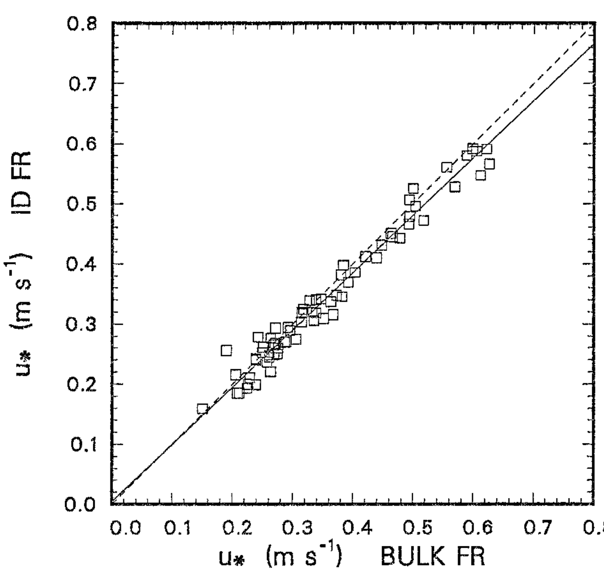

FIG. 8. As in Fig. 3 except for FR inertial-dissipation versus FR bulk u_* values.

TABLE 3. Uncertainties used in the HEXMAX-specific error analysis for the ship (FR) and tower (MPN) platforms and the inertial-dissipation (ID), bulk, and direct covariance (DC) methods.

Parameter	Uncertainty	Platform, method
Wind speed U	$\delta U = \pm 5\% \times U$	FR ID, bulk
Air temperature T_{air}	$\delta T_{air} = +0.3°C$	FR ID, bulk
Sea temperature T_{sea}	$\delta T_{sea} = \pm 0.5°C$	FR ID, bulk
Relative humidity RH	$\delta RH = \pm 5\%$	FR ID, bulk
Measurement height z	$\delta z = \pm 0.5$ m	FR ID, bulk
Drag coefficient C_{DN10}	$\delta C_{DN10} = \pm 5\% \times C_{DN10}$	FR bulk
Wind speed U	$\delta U = \pm 2.5\% \times U$	MPN ID
Monin–Obukhov length L	$\delta L = \pm 25\% \times L$	MPN ID
Measurement height z	$\delta z = \pm 0.1$ m	MPN ID
Wind spectra $S_u(f)$	$\delta S_u(f) = \pm 8\% \times S_u(f)$	MPN/FR ID
Von Kármán's constant k	$\delta k = \pm 0.01$	MPN/FR ID, FR bulk
Wind profile function Φ_M	$\delta \Phi_M = \pm 5\% \times \Phi_M$	MPN/FR ID, FR bulk
Kolmogorov constant α_e	$\delta \alpha_e = \pm 0.01$	MPN/FR ID
Wind covariance $u'w'$	$\delta u'w' = \pm 2\% \times u'w'$	MPN DC
Finite averaging η	Eqs. (10) and (11)	MPN DC

is smaller for this comparison than between the FR bulk values and the MPN ID and covariance u_* values, most likely because the same mean measurements were used to compute both FR values. These results demonstrate that for the conditions of this study, the inertial-dissipation method of determining the wind stress was superior to the bulk method.

From the summary in Table 2 it can be seen that the observed scatter in the MPN covariance comparisons with both the FR ID and bulk u_* values (9.6% and 10.7%, respectively) is larger than the scatter in the MPN ID comparisons with the FR ID and bulk data (6.7% and 8.6%, respectively). This suggests that the errors are larger in the MPN covariance measurements than the MPN ID u_* determinations, although it is possible that the larger scatter in the covariance measurements is due to low-frequency turbulent fluctuations being resolved by the covariance method and not by the ID method.

5. Error analysis

In this section a detailed error analysis is performed upon the HEXMAX ship and tower measurements. The uncertainties assumed for the parameters used to compute the u_* values are discussed in section 5a. A discussion of the methods used in the error analysis is presented in section 5b. An error analysis specific to the conditions of the HEXMAX experiment is conducted in section 5c, in order to explain the observed scatter in the HEXMAX data by estimating the errors associated with each u_* population involved in a comparison. Finally, in section 5d, an error analysis for general conditions not specific to the HEXMAX experiment is conducted in order to estimate the errors associated with wind stress determinations obtained using the different methods and measurement platforms.

a. Estimated uncertainties used in the error analysis

1) MEASUREMENT ERRORS

Measurement errors are associated with problems in the physical measurement of a parameter, due to such factors as sensor accuracy and sensitivity, calibration errors, flow distortion, etc. The assumed measurement errors used in this analysis are presented in Table 3. An error of 8% was assumed for both the MPN sonic anemometer and FR hot-film wind speed variance spectra $S_u(f)$. This assumed error is slightly lower than the 10% error estimated for MPN variance spectra by Edson et al. (1991). The estimated 8% error is based on a comparison between many concurrent shipboard measurements of $S_u(f)$ made by the NPS group with adjacent sensors. This assumed error is also supported by Yelland et al. (1994), who observed 3%–12% differences in $S_u(f)$ measurements made by four anemometers on the foremast of a research vessel. We used the same assumed measurement error of 2% as Edson et al. (1991) for the MPN $-\langle u'w' \rangle$ covariance.

The errors assumed for mean measurements are based upon comparisons between different sensors on many cruises and are very similar to the sensor errors used by Blanc (1986). The assumed 25% error in MPN ID Monin–Obukhov length values was determined by examining the differences between MPN ID, MPN covariance, FR ID, and FR bulk L values. The assumed measurement errors used in this study are based primarily on the estimated accuracy of the various sensors in a marine environment. Since the sensors were well exposed on the FR, and only data collected with favorable winds from the bow were used, we feel that the ship's influence on the measurements was minimal and can be included within the assumed errors.

2) FINITE AVERAGING ERRORS

Finite averaging errors are associated with estimating ensemble averages of turbulence statistics (variances and covariances) by finite time averages. Following Wyngaard (1973), Edson et al. (1991) estimated the fractional error η due to approximating ensemble averages of the covariance $\langle u'w' \rangle$ with finite time averages by

$$\eta = 0.39\left[\frac{z \ \mathrm{var}(u'w')}{T_a(u'w')^{1/2}}\right]^{1/2} \quad (10)$$

for the HEXMAX MPN measurements. Here z is the measurement height, T_a is the averaging interval, and $\mathrm{var}(u'w')$ is the variance of $u'w'$, given by (Edson et al. 1991)

$$\mathrm{var}(u'w') = \begin{cases} 7(1 + 5|z/L|^{2/3}), & z/L < 0 \\ 10, & z/L > 0. \end{cases} \quad (11)$$

Note that finite averaging errors decrease with increasing averaging intervals, as intuitively expected. Equations (10) and (11) were used to estimate the errors in the MPN covariance u_* values due to finite averaging. Edson et al. (1991) demonstrated that the errors in streamwise wind speed variance averages [associated with $S_u(f)$ estimates] are approximately 40% the magnitude of the errors in covariance averages for the same averaging interval and measurement height. In this study we have assumed, as did Edson et al. (1991), that the errors in the MPN and FR $S_u(f)$ values due to finite averaging are contained within the assumed 8% measurement error.

3) Method errors

Method errors are associated with uncertainties inherent in the method employed, due to simplifying assumptions that must be made and to uncertainties in the empirical constants and functions that are used. Errors in the inertial-dissipation method due to deviations from the assumed balance between TKE dissipation and production were estimated by assuming an uncertainty in the effective Kolmogorov constant α_e. This is done because α_e represents the value the actual Kolmogorov constant would have if a TKE balance in fact exists; therefore any change in its value has the effect of representing a deviation from a TKE balance. We have used the value and uncertainty (0.55 ± 0.01) found by Edson et al. (1991) in their determination of α_e from the HEXMAX MPN data. This small uncertainty reflects the fact that the value of α_e used in this study was determined explicitly by finding the best fit between the MPN covariance and inertial-dissipation u_* measurements.

As discussed in section 3c, errors in bulk methods can be due to errors in the original measurements used to derive the drag coefficient and also to differences between the conditions existing when the bulk formulation is applied and the average conditions that occurred when the drag coefficient was originally determined. Since the HEXMAX measurement site was essentially the same for the ship and the tower in this study, the assumed 5% error in C_{DN10} was determined by examining the scatter in the original measurements used to determine the Smith et al. (1992) formulations.

Both the bulk and inertial-dissipation methods depend upon the dimensionless wind profile function Φ_M, and on the von Kármán constant k. We have assumed a 5% relative error in Φ_M, as estimated by Edson et al. (1991) from examining the differences between several sets of empirical forms for the function. An error of ± 0.01 was assumed for k, based on the review by Frenzen and Vogel (1995).

b. Error analysis methods

The estimated relative errors in the FR and MPN ID and the FR bulk u_* values were computed using the assumed uncertainties listed in Table 3 and the error analysis method described in the appendix. The relative errors in the MPN direct covariance u_* values were estimated by summing the finite averaging error and the covariance measurement error, and then dividing by 2 since we are interested in the error in u_* [equivalent to $(-\langle u'w' \rangle)^{1/2}$] rather than $-\langle u'w' \rangle$.

The "predicted" scatter P was computed by determining the mean value of the square root of the sum of the squares of the estimated relative errors in the two u_* values being compared:

$$P = \frac{1}{N}\sum_{i=1}^{N}\left[\left(\frac{\delta X}{X}\bigg|_i\right)^2 + \left(\frac{\delta Y}{Y}\bigg|_i\right)^2\right]^{1/2}, \quad (12)$$

where X and Y represent the two u_* populations being compared and N is the number of data pairs in the comparison. The predicted scatter provides an estimate of the amount of scatter that should be observed in the u_* comparisons due to systematic and random errors in both populations being compared.

The error analyses were conducted differently for each comparison in order to attempt to explain the observed scatter O through the predicted scatter P. When comparing two u_* populations derived from methods that depend upon the same constants (k, α) and/or functions (Φ_M, C_{DN10}, C_{TN10}), the uncertainties in these parameters were not included in the error analysis. This was done because uncertainties in the constants and functions would not increase the scatter in a comparison because the same constants and functions were used for computing both populations. When comparing two u_* populations that depend upon measurements from the same sensors (FR bulk versus ID and MPN ID versus covariance comparisons), the uncertainties due to the assumed measurement errors were subtracted from each other in order to approximate the tendency of the errors to cancel.

c. HEXMAX error analysis results

The predicted scatter values for the friction velocity comparisons are presented in Table 2. The percentage

TABLE 4. Uncertainties used in the general error analysis, where different from the HEXMAX-specific analysis.

Parameter	Uncertainty	Platform/method
Kolmogorov constant α_e	$\delta\alpha_e = \pm 0.05$	FR/MPN ID
Monin–Obukhov length L	$\delta L = \pm 100\% \times L$	MPN ID
Drag coefficient C_{DN10}	$\delta C_{DN10} = \pm 25\% \times C_{DN10}$	FR bulk

of the predicted scatter due to the estimated errors in each of the two u_* populations in a comparison is also shown, where the first value, X% of P, refers to the u_* population listed at the top of the columns, and the second value, Y% of P, refers to the u_* population listed to the left of the rows. As seen in Table 2, the difference between the observed and predicted scatter was 0.3% or less for every u_* comparison. This remarkable agreement indicates that the methods and uncertainties used in the error analysis are reasonable and that the observed scatter between the u_* populations is in fact due to measurement, finite averaging, and method errors that were similar in magnitude to those assumed in the error analysis.

The error analysis results presented in Table 2 indicate that errors in the MPN covariance measurements contributed much more to the combined scatter in comparisons with both the MPN and FR ID values, and roughly the same amount as the FR bulk u_* values. A larger amount of the scatter in the FR ID versus MPN ID comparison was due to uncertainties in the shipboard measurements, since the assumed measurement errors were larger for the FR. Uncertainties in the FR bulk u_* values contributed much more to the combined scatter in comparisons with the MPN ID and FR ID values. These results indicate that errors were largest in the FR bulk u_* values, followed in descending order by the MPN covariance, the FR ID, and the MPN ID u_* values.

d. General error analysis results

The excellent agreement between the observed and predicted scatter for every u_* comparison indicates that the error analysis methods employed are sound. This provided motivation to conduct a further analysis to estimate the errors associated with wind stress determinations under more general conditions. This general error analysis was conducted using the same methods as outlined above, but with different assumed uncertainties in some cases from the HEXMAX-specific values, as indicated in Table 4. The results of the general error analysis are summarized in Table 5. The ''predicted error'' E is the mean value of the relative error estimates computed for each u_* value in a given population. The percentages of the predicted error due to uncertainties in each constituent parameter used to compute the u_* values are also listed in Table 5.

TABLE 5. Results of the general error analysis, including the mean predicted error in the friction velocity u_* measurements, E, and the percentage of E due to assumed uncertainties in the parameters used to compute u_*. Results are presented for the ship (FR) and tower (MPN) platforms and the inertial-dissipation (ID), bulk, and direct covariance (DC) methods.

	FR ID	MPN ID	FR bulk	MPN DC
Predicted error in u_*, E(%)	7.3	6.8	13.9	7.5
Percentage of E due to uncertainty in				
Wind speed, δU	5.7	1.5	27.1	—
Air temperature, δT_{air}	3.1	—	0.3	—
Sea temperature, δT_{sea}	6.9	—	1.0	—
Relative humidity, δRH	0.1	—	0.0	—
Monin–Obukhov length, δL	—	9.2	—	—
Measurement height, δz	3.6	0.8	0.1	—
Von Kármán's constant, δk	1.4	1.5	0.0	—
Wind profile function, $\delta\Phi_M$	4.7	5.7	0.4	—
Wind spectra, $\delta S_u(f)$	32.3	35.3	—	—
Kolmogorov constant, $\delta\alpha_e$	42.0	45.9	—	—
Drag coefficient, δD_{DN10}	—	—	71.2	—
Wind covariance, $\delta(u'w')/2$	—	—	—	13.8
Finite averaging, $\eta/2$	—	—	—	86.2

1) INERTIAL-DISSIPATION METHOD

In the general error analysis an uncertainty of ± 0.05 was assumed for the Kolmogorov constant in order to cover the range from a small true value of the constant (0.5) to a large value of the effective Kolmogorov constant (0.6), as seen from the discussion in section 3b. Assuming 0.55 is the actual value of the effective Kolmogorov constant that should be used under given conditions, an uncertainty of ± 0.05 accounts for a TKE dissipation–production imbalance of roughly $\pm 14\%$. The general error analysis resulted in a predicted 7.3% error in shipboard ID u_* determinations, leading to an error of about 15% in wind stress values. The predicted error for the tower ID u_* determinations was 6.8%, which is slightly smaller than the shipboard error due to the assumed more accurate mean measurements and measurement height on the tower.

The assumed uncertainty in the effective Kolmogorov constant, representing a deviation from a TKE balance, contributed the most to the predicted error in both the shipboard and tower u_* values, 42% and 46%, respectively. The assumed error in the wind speed variance spectra $S_u(f)$ also contributed a large amount to the predicted error, 32% for the ship and 35% for the tower. Errors in the mean air–sea measurements, upon which z/L strongly depends, contributed much smaller amounts to the predicted error in ID u_* values, due to the slowly varying behavior of the stability function $\Phi_M - z/L$ in near-neutral conditions. In strongly stable or unstable conditions, when $\Phi_M - z/L$ varies much more rapidly with z/L, errors in the mean measurements would likely lead to larger errors in the resulting u_* values. Uncertainties in von Kármán's constant and the dimensionless profile function contributed only minimally to the predicted errors in ID u_* determinations.

The above results indicate that the most promising means to improve the ID method lie primarily in obtaining a better understanding of the terms in the TKE budget and of the effective Kolmogorov constant, and in improving the accuracy of wind variance spectra determination techniques.

2) Bulk method

An uncertainty of 25% was assumed for C_{DN10} in the general error analysis, determined by comparing the differences between various shallow-water C_{DN10} versus U_{N10} relationships (Smith 1988; Geernaert et al. 1986; Smith et al. 1992) and by examining the scatter in the original measurements used to determine these relationships. The error analysis resulted in a predicted 13.9% error in shipboard bulk u_* determinations, leading to errors of about 28% in the wind stress. These errors were due almost entirely to the assumed uncertainties in C_{DN10}, which accounted for 71% of the predicted error, and in the mean wind speed, which accounted for 27% of the predicted error. Errors in the other mean air–sea measurements and uncertainties in the von Kármán constant and the dimensionless profile function contributed only negligible amounts to the predicted error in bulk u_* values. It is likely that future improvements in bulk u_* determinations will result from continuing efforts to include the effects of wave age, fetch, sea state, gustiness, and other factors on the drag coefficient, in addition to the effects of wind speed and stability.

3) Direct covariance method

The predicted error for the MPN direct covariance u_* values was 7.5%, which is very similar to the estimated error in shipboard ID u_* determinations. The assumed errors due to approximating ensemble averages by finite time averages accounted for the great majority of the predicted error in covariance u_* values, 86%, as opposed to the actual covariance measurement errors, which accounted for only 14% of the predicted error. By using longer averaging intervals, the finite averaging errors should decrease, as long as conditions remain near stationary. It should be remembered that the covariance measurements used in this study were carefully corrected for flow distortion effects, although in many applications such corrections may not be feasible. Therefore, it appears that the best strategy to improve the accuracy of covariance wind stress measurements is to use long averaging intervals and to minimize the effects of flow distortion through improved sensor design and by using well-exposed sensor locations relative to supporting structures and platforms. The development of flow distortion correction models where possible, such as those applied to the HEXMAX MPN covariance measurements, may also improve the accuracy of covariance wind stress determinations.

6. Conclusions

The very strong agreement between the ship inertial-dissipation and tower friction velocity measurements demonstrates that the wind stress can be measured on a ship using the inertial-dissipation method with a high degree of accuracy. The ship inertial-dissipation u_* values agreed better with both the tower covariance and dissipation measurements than the ship bulk values, despite the fact that the bulk formulation was determined from covariance measurements made on the MPN tower during HEXMAX. The ship inertial-dissipation friction velocity values also exhibited less scatter than both the ship bulk and tower covariance measurements. These results demonstrate that when the effects of flow distortion are minimized, such as by placing sensors in well-exposed locations and using only favorable wind directions, the inertial-dissipation method of determining the wind stress is superior to the bulk method.

The error analysis conducted in this study indicates that the wind stress can be determined by the inertial-dissipation method on a ship with an accuracy of about 15% in near-neutral conditions, as compared to an accuracy of roughly 30% for the bulk method. The estimated 15% accuracy in shipboard inertial-dissipation wind stress determinations was comparable to the accuracy of direct covariance measurements obtained on a stable tower. In many ways this analysis represents a ''best case'' for the covariance method, however, since it has been shown to be much more influenced by flow distortion than the inertial-dissipation method. The covariance measurements used in this study were carefully corrected for flow distortion effects at the MPN boom location, while in many applications such corrections will be very difficult or impossible to implement. In addition, the use of the covariance method on ships and buoys requires corrections for platform motion, which introduce further sources of error and greatly increase the difficulty and cost of the measurements. All these factors demonstrate that the inertial-dissipation method is the best method available at present for determining the wind stress from a ship. Continuing research toward a better understanding of the TKE budget and the Kolmogorov constant, as well as improved measurement techniques, will further increase the accuracy of the inertial-dissipation method in the future.

Acknowledgments. The authors would like to thank the scientists and crews on board the MPN platform and the RRS *Frederick Russell* for their efforts in data collection during the HEXMAX experiment. Special thanks are due to Peter Taylor, chief scientist on the *Frederick Russell*, and Chris Fairall, Patrice Mestayer, and Soren Larsen of the HEXIST group. Funding for this study was provided by grants from the Marine Meteorology Division of the Office of Naval Research to NPS and to WHOI (Grants N00014-85-K-0250 and N00014-85-K-0123). The NPS data analysis was supported by the NRL-Stennis Space Center, Remote Sensing Applications Branch.

APPENDIX

Error Analysis Methodology

In this study we have estimated the errors in friction velocity determinations using the error analysis procedures outlined by Blanc (1986). This approach involves estimating the error in u_* by examining the differences between the u_* value computed assuming no errors in the constituent parameters and the u_* values computed assuming both a positive and a negative error in each constituent parameter. For example, assuming u_* is a function of parameters A and B, the best estimate of u_* is first computed by assuming there are no errors in A or B;

$$u_{*(A,B)} = f(A, B). \tag{A1}$$

Then u_* is computed with each of the assumed errors ($A \pm \delta A$, $B \pm \delta B$) considered one at a time:

$$\begin{aligned} u_{*(A+\delta A,B)} &= f(A + \delta A, B) \\ u_{*(A-\delta A,B)} &= f(A - \delta A, B) \\ u_{*(A,B+\delta B)} &= f(A, B + \delta B) \\ u_{*(A,B-\delta B)} &= f(A, B - \delta B). \end{aligned} \tag{A2}$$

Since an error in a parameter cannot be greater and lower than the actual value simultaneously, the differences between the value of u_* computed assuming no error and the values of u_* computed assuming a positive and negative error are averaged together to estimate the typical error in u_* due to an error in the parameter;

$$\begin{aligned} \delta u_{*(A)} &= \left(\frac{|u_{*(A+\delta A,B)} - u_{*(A,B)}| + |u_{*(A-\delta A,B)} - u_{*(A,B)}|}{2}\right) \\ \delta u_{*(B)} &= \left(\frac{|u_{*(A,B+\delta B)} - u_{*(A,B)}| + |u_{*(A,B-\delta B)} - u_{*(A,B)}|}{2}\right). \end{aligned} \tag{A3}$$

If parameters A and B are independent of each other and the errors in A and B are uncorrelated, then the most probable relative (percentage) error in u_* is estimated by taking the square root of the sum of the squares of the errors in u_* due to parameters A and B, dividing by the best estimate of u_* computed assuming there are no errors in A and B, and multiplying by 100 to express as a percentage:

$$\frac{\delta u_*}{u_*} = 100 \times \frac{\left[(\delta u_{*(A)})^2 + (\delta u_{*(B)})^2\right]^{1/2}}{u_{*(A,B)}}. \tag{A4}$$

REFERENCES

Anderson, R. J., 1993: A study of wind stress and heat flux over the open ocean by the inertial-dissipation method. *J. Phys. Oceanogr.,* **23,** 2153–2161.

Blanc, T. V., 1986: The effect of inaccuracies in weather-ship data on bulk-derived estimates of flux, stability and sea-surface roughness. *J. Atmos. Oceanic Technol.,* **3,** 12–26.

Bradley, E. F., R. A. Antonia, and A. J. Chambers, 1981: Turbulence Reynolds number and the TKE balance in the atmospheric surface layer. *Bound.-Layer Meteor.,* **21,** 183–197.

Champagne, F. H., C. A. Friehe, J. C. LaRue, and J. C. Wyngaard, 1977: Flux measurements, flux estimation techniques, and fine-scale turbulence measurements in the unstable surface layer over land. *J. Atmos. Sci.,* **34,** 515–530.

Deacon, E. L., 1988: The streamwise Kolmogorov constant. *Bound.-Layer Meteor.,* **42,** 9–17.

Edson, J. B., C. W. Fairall, P. G. Mestayer, and S. E. Larsen, 1991: A study of the inertial-dissipation method for computing air-sea fluxes. *J. Geophys. Res.,* **96,** 10 689–10 711.

Fairall, C. W., and J. B. Edson, 1994: Recent measurements of the dimensionless turbulent kinetic energy dissipation function over the ocean. Preprint, *Second Int. Conf. on Air–Sea Interaction and Meteorology and Oceanography of the Coastal Zone,* Lisbon, Portugal, Amer. Meteor. Soc., 224–225.

——, ——, S. E. Larsen, and P. G. Mestayer, 1990: Inertial-dissipation air–sea flux measurements: A prototype system using realtime spectral computations. *J. Atmos. Oceanic Technol.,* **7,** 425–453.

Frenzen, P., and C. A. Vogel, 1992: The turbulent kinetic energy budget in the atmospheric surface layer: A review and an experimental reexamination in the field. *Bound.-Layer Meteor.,* **60,** 49–76.

——, and ——, 1995: On the magnitude and apparent range of variation of the von Karman constant in the atmospheric surface layer. *Bound.-Layer Meteor.,* **72,** 371–392.

Garratt, J. R., 1972: Studies of turbulence in the surface layer over water (Lough Neagh), Part II: Production and dissipation of temperature and velocity fluctuations. *Quart. J. Roy. Meteor. Soc.,* **98,** 642–657.

——, 1992: *The Atmospheric Boundary Layer.* Cambridge University Press, 316 pp.

Geernaert, G. L., K. B. Katsaros, and K. Richter, 1986: Variation of the drag coefficient and its dependence on sea state. *J. Geophys. Res.,* **91,** 7667–7679.

——, K. L. Davidson, S. E. Larsen, and T. M. Mikkelson, 1988: Wind stress measurements during the tower ocean wave and radar dependence experiment. *J. Geophys. Res.,* **93,** 13 913–13 924.

Hogstrom, U., 1990: Analysis of turbulence structure in the surface layer with a modified similarity formulation for near neutral conditions. *J. Atmos. Sci.,* **47,** 1949–1972.

——, 1996: Review of some basic characteristics of the atmospheric surface layer. *Bound.-Layer Meteor.,* **78,** 215–246.

Khalsa, S., and J. A. Businger, 1977: The drag coefficient as determined by the dissipation method and its relation to intermittent convection in the surface layer. *Bound.-Layer Meteor.,* **12,** 273–297.

Kraus, E. B., and J. A. Businger, 1994: *Atmosphere–Ocean Interaction.* Oxford University Press, 352 pp.

Large, W. G., and S. Pond, 1981: Open ocean momentum fluxes in moderate to strong winds. *J. Phys. Oceanogr.,* **11,** 324–336.

McBean, G. A., and J. A. Elliott, 1975: The vertical transports of kinetic energy by turbulence and pressure in the boundary layer. *J. Atmos. Sci.,* **32,** 753–766.

——, R. W. Stewart, and M. Miyake, 1971: The turbulent energy budget near the surface. *J. Geophys. Res.,* **76,** 6540–6549.

Oncley, S. P., T. W. Horst, A. Praskovsky, and J. M. Wilczak, 1995: The TKE budget from the FLAT experiment. Preprint, *11th Symp. on Boundary Layers and Turbulence,* Charlotte, NC, Amer. Meteor. Soc., 5–8.

——, C. A. Friehe, J. C. LaRue, J. A. Businger, E. C. Itsweire, and S. S. Chang, 1996: Surface-layer fluxes, profiles, and turbulence measurements over uniform terrain under near-neutral conditions. *J. Atmos. Sci.,* **53,** 1029–1044.

Oost, W. A., C. W. Fairall, J. B. Edson, S. D. Smith, R. J. Anderson, J. A. B. Wills, K. B. Katsaros, and J. DeCosmo, 1994: Flow distortion calculations and their application in HEXMAX. *J. Atmos. Oceanic Technol.,* **11,** 366–386.

Pond, S., G. T. Phelps, J. E. Pasquin, G. McBean, and R. W. Stewart, 1971: Measurements of the turbulent fluxes of momentum, moisture and sensible heat over the ocean. *J. Atmos. Sci.,* **28,** 901–917.

Smith, S. D., 1988: Coefficients for sea surface wind stress, heat flux, and wind profiles as a function of wind speed and temperature. *J. Geophys. Res.,* **93,** 15 467–15 472.

——, and Coauthors, 1992: Sea surface wind stress and drag coefficients: The HEXOS results. *Bound.-Layer Meteor.,* **60,** 109–142.

Vogel, C. A., and P. Frenzen, 1992: A new study of the TKE budget in the surface layer. Part II: The dissipation function and divergent transport terms. Preprint, *10th Symp. on Turbulence and Diffusion,* Portland, OR, Amer. Meteor. Soc., 161–164.

Wyngaard, J. C., 1973: On surface layer turbulence. *Workshop on Micrometeorology,* D. A. Haugen, Ed., Amer. Meteor. Soc., 101–149.

——, and O. R. Cote, 1971: The budgets of turbulent kinetic energy and temperature variance in the atmospheric surface layer. *J. Atmos. Sci.,* **28,** 190–201.

Yelland, M. J., and P. K. Taylor, 1996: Wind stress measurements from the open ocean. *J. Phys. Oceanogr.,* **26,** 541–558.

——, ——, I. E. Consterdine, and M. H. Smith, 1994: The use of the inertial dissipation technique for shipboard wind stress determination. *J. Atmos. Oceanic Technol.,* **11,** 1093–1108.